Opto-Electronic Science

Supplementary information

2022, Vol. 1, No. 9

DOI: 10.29026/oes.2022.220004

100 Hertz frame-rate switching three-dimensional orbital angular momentum multiplexing holography via cross convolution

Weijia Meng[1,2], Yilin Hua[1,2]*, Ke Cheng[1,2], Baoli Li[1,2], Tingting Liu[1,2], Qinyu Chen[1,2], Haitao Luan[1,2], Min Gu[1,2]* and Xinyuan Fang[1,2]*

[1]Institute of Photonic Chips, University of Shanghai for Science and Technology, Shanghai 200093, China; [2]Centre for Artificial-Intelligence Nanophotonics, School of Optical-Electrical and Computer Engineering, University of Shanghai for Science and Technology, Shanghai 200093, China.

*Correspondence: YL Hua, E-mail: huayilin@usst.edu.cn; M Gu, E-mail: gumin@usst.edu.cn; XF Fang, E-mail: xinyuan.fang@usst.edu.cn

This file includes:

Supplementary information for this paper is available at https://doi.org/10.29026/oes.2022.220004

Section 1: Generation of OAM selective and OAM multiplexing holograms

Generation of an OAM selective hologram can be illustrated on the inset map above the hologram in Fig. 2(a) in the main text. The Fourier transform hologram can be expressed as:

$$H(x,y) = \mathcal{F}\{O(u,v)\}\ , \tag{S1}$$

where (x,y) and (u,v) represent the orthogonal coordinates in the hologram plane and the image plane and $O(u,v)$ is the target image.

A helical phase of $\exp(\mathrm{j}l_{\mathrm{sn}}\varphi_1)$ should be superposed on this hologram to form an OAM selective hologram, where l_{sn} is the topological charge of the OAM mode and φ_1 is the azimuth in the polar coordinates. After preparing a series of OAM selective holograms with individual OAM charges, the procedure of packing many images into a single OAM multiplexing hologram becomes a trivial superposition operation[S1,S2] of these OAM selective holograms can be described as:

$$H_N(\xi,\eta) = \sum_{sn=1}^{N} \mathcal{F}\{O(u,v)\}\exp(\mathrm{j}l_{\mathrm{sn}}\varphi_1)\ , \tag{S2}$$

where N is the total number of the OAM selective holograms.

Section 2: The influence of an OAM selective hologram illuminated by the mismatched OAM on the reconstructed image

To illustrate the situation of decoding an OAM selective hologram with the mismatched decoding OAM charge, an OAM selective hologram of the letter "l" is encoded with an OAM charge ($l_{\mathrm{sn}} = 1$). According to the OAM selection rule of the cross convolution theorem, holographic reconstructed image can appear at the first diffraction order (b=1) only when the decoding OAM charge satisfies $l_{\mathrm{dm}} = -1$. We compare two situations of decoding the image with correct and mismatched decoding OAM charges of $l_{\mathrm{dm}} = -1$ and $l_{\mathrm{dm}} = -2$, as shown in Fig. S1(a) and Fig. S1(b), respectively. We can clearly see that when the correct decoding OAM charge is applied, each pixel of the reconstructed image exhibits a Gaussian mode with a bright light intensity distribution. When the mismatched decoding OAM charge is applied, the letter "l" can still be reconstructed which is consisted of pixels with doughnut type (as can be seen in the enlarged insert map on the upper right corner) while the overall brightness of the reconstructed image is really low. The decoding OAM charge is measured using the astigmatic transformation patterns[S3] induced by a tilted spherical lens in which the number of dark lines and inclination angle can judge the OAM value and symbol (as can be seen in inset map on the upper right corner with $l_{\mathrm{dm}} = -2$).

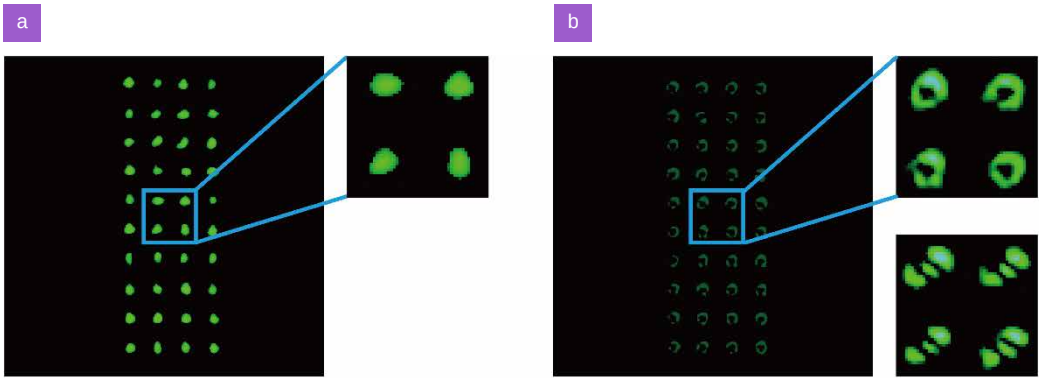

Fig. S1 | Results of illuminating OAM selective hologram with correct and mismatched decoding OAM charge.

Section 3: The OAM spacing to encode information for improving signal to noise ratio

In the experiment of high-speed information retrieval from an OAM multiplexing hologram. We demonstrate the rapid retrieval of the first 100 significant digits of π, in which 10 types of Arabic numerals ranging from 0 to 9 are encoded with different OAM charges in an OAM multiplexing hologram. To analyse the impact of OAM spacing on the signal-to-noise ratio (SNR) of retrieval each image of the Arabic numerals, we simulate the performance of information re-

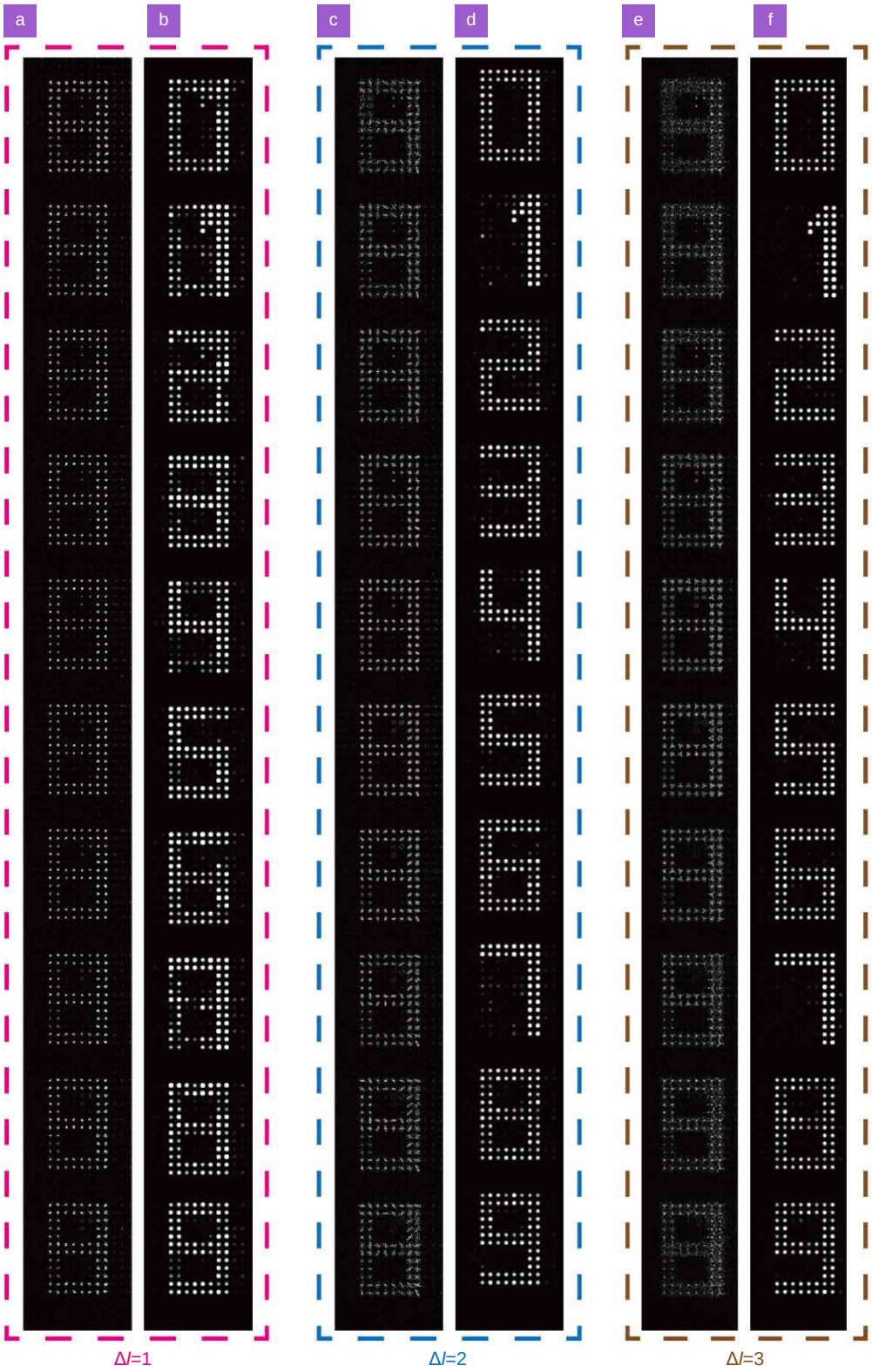

Fig. S2 | Simulated results of reconstruction of various images of Arabic numerals with different encoding OAM spacing.

trieval with different OAM spacing. Three typical OAM helical mode intervals are simulated with two different configurations with and without a mode-selective aperture array. The effect of the mode-selective aperture array is to enhance the SNR of the OAM selectivity through selecting the pixels with the fundamental Gaussian mode and eliminating pixels with other shape[S2].

Figure S2 shows the performance of reconstruction of various Arabic numerals with different encoding OAM spacing. The results are simulated at b=1 (the first diffraction order) with the correct OAM selection rule. Figure S2(a), S2(c) and S2(e) are the results with an OAM spacing of Δl=1, 2 and 3 without a mode-selective aperture array, and Fig. S2(b), S2(d) and S2(f) are the results with a mode-selective aperture array corresponding to Fig. S2(a), S2(c) and S2(e) respectively. We can see that with the increasing of the encoding OAM spacing, both results of the image reconstruction have better performance whether the selective aperture array is applied or not. However, when the OAM spacing is too small, we find that the signal to noise ratio is low even with a mode-selective aperture array. The average SNR of these 10 images with different OAM spacing is calculated to be 5.30 (Δl=1), 8.18 (Δl=2) and 9.59 (Δl=3) when the mode-selective aperture array is applied. An improvement on SNR is found with the increasing of encoding OAM spacing. Therefore, in order to obtain good imaging results experimentally, we choose the helical mode interval equal to 10.

Section 4: The dependence of the encoded OAM capacity on the hologram resolution

In OAM holography, the sampling constant is proportional to the OAM helical mode index[S2]. That is to say the sampling distance increases as the helical mode index increases. The maximum diffraction angle of a digital hologram can be expressed as $\beta_{\max} = \arctan(\lambda/2p)$, where λ is the wavelength of light and p is the size of a single pixel of the hologram. According to ray optics, the maximum size of the reconstructed image is $D_{\max} = 2f\tan(\beta_{\max}) - H$, where f is the focal length of the Fourier lens and H is the size of the hologram. Therefore, the maximum size determines the maximum helical mode index ($l_{\max}$) that can be used when considering the limit case that sampling distance is equal to the value of $D_{\max}$. In an OAM multiplexing hologram, when the appropriate OAM spacing (Δl) is fixed, the number of frames that can be encoded is then determined by $l_{\max}/\Delta l$. Therefore, we can plot the relationship between the pixel size of the hologram and the maximum mode index to illustrate the capacity of the maximum frame numbers of images decided by the resolution of the device that records holograms. It is not difficult to see that as the pixel size of the hologram decreases, the maximum mode index increases rapidly, so that a higher frame number of images can be recorded with a metasurface.

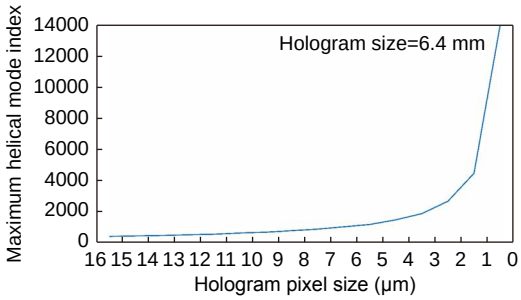

Fig. S3 | The maximum helical mode index dependence on the pixel size of the hologram.

Section 5: The principle of 3D OAM holography

As shown in Fig. S4(a), it describes a real 3D object (airplane) consisting of a large number of discrete images. In order to realize 3D OAM holographic display, each image describes a slice of a 3D object in a specific plane, and all these images should be encoded into a single hologram. To implement 3D OAM-selective holography (Fig. S4(b)), all images are first sampled through the space-frequency domain. It is worth noting that the spatial frequency of the helical mode determines the minimum sampling spacing, which is larger compared to previous holography. Next a series of parabolic phases are used so that different images can be focused onto different z_i coordinates in the reconstruction process. Then we use a same helical mode index to achieve the OAM-selective holograms. Finally, through a simple stacking operation, a 3D OAM-selective hologram is formed, and can only appear with opposite helical mode index according to the OAM selection rule. Therefore, the hologram has a form of:

$$H_N(x,y) = \sum_{n=1}^{N}\left\{\sum_{u=1}^{M}\sum_{v=1}^{M} O_n(u,v)\exp\left[\mathrm{j}2\pi(ux+vy)\right]\cdot\exp(\mathrm{j}l_s\varphi)\right\}\cdot\exp\left[-\mathrm{j}\frac{\pi}{\lambda z_n}(x^2+y^2)\right], \tag{S3}$$

where $O_n(u,v)$ stands for complex amplitude distribution of the N images and z_n is the position where the image is

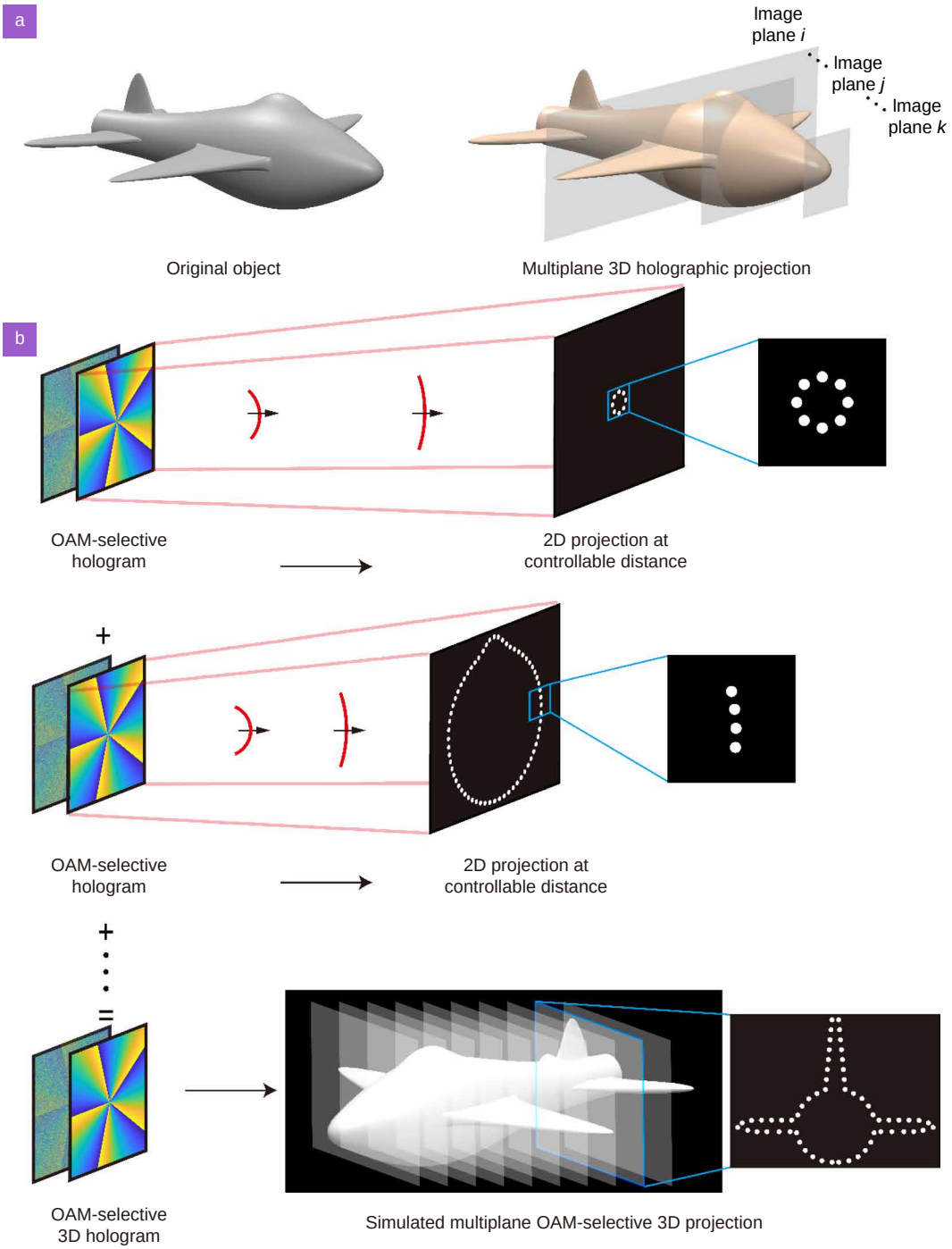

Fig. S4 | The principle of 3D OAM holography.

projected at.

To construct an OAM selective hologram for a true 3D object, the increasing of the sampling distance proportional to the spatial frequency of the OAM helical mode is essential. This leads to a reduction of the valid pixel numbers of an image of each plane. As described by the reference[S1], each image is considered as a *N*-dimensional vector. Therefore, the reduction of valid pixel numbers leads to the decline of the dimension directly. As a result, the orthogonality of these vectors degenerates as the dimension decreases and the cross talk between the reconstructed images cannot be eliminated effectively. Therefore, the increase of the superposed 2D images at different image depths in our system will bring large crosstalk, limiting the performance of 3D OAM holography to reconstruct a true object with a continuous *z* profile.

Section 6: The description of the supplement video of the fast switching OAM multiplexing holography via cross convolution

This is a supplement video of an OAM multiplexing holography via cross convolution to deliver the first 100 significant digits of π. Among them, the first 10 frames are the refresh rate of 1 Hz, and the rest are refresh rate at a high speed of 100 Hz.

References

S1. Makey G, Yavuz Ö, Kesim DK, Turnalı A, Elahi P et al. Breaking crosstalk limits to dynamic holography using orthogonality of high-dimensional random vectors. *Nat Photonics* **13**, 251–256 (2019).

S2. Fang XY, Ren HR, Gu M. Orbital angular momentum holography for high-security encryption. *Nat Photonics* **14**, 102–108 (2020).

S3. Kotlyar VV, Kovalev AA, Porfirev AP. Astigmatic transforms of an optical vortex for measurement of its topological charge. *Appl Opt* **56**, 4095–4104 (2017).